Applied Water Science (2023) 13:84
https://doi.org/10.1007/s13201-023-01891-9

ORIGINAL ARTICLE

Groundwater quality assessment for domestic and agricultural purposes using GIS, hydrochemical facies and water quality indices: case study of Rafsanjan plain, Kerman province, Iran

Mohadeseh Hosseininia[1] · **Reza Hassanzadeh**[2]

Received: 26 July 2022 / Accepted: 10 February 2023 / Published online: 28 February 2023

Abstract

This paper investigates the suitability of groundwater for domestic and agricultural use in the Rafsanjan plain, southwest part of the Daranjir–Saghand basin, Iran. Fifty-five groundwater samples were collected and analyzed by six methods including the water quality index (WQI), Schoeller diagram, irrigation water quality (IWQ) parameters, Piper diagram, US salinity diagram and Wilcox diagram. The spatial distribution maps of chemical parameters and groundwater quality indices were plotted using the IDW method in GIS. The results showed a low concentration of major ions in the southeastern part and a high concentration from the central part towards northwestern part of the plain. The concentration of major ions in groundwater was strongly affected by groundwater flow, geological setting and the existence of the evaporative layers in the studied area. Moreover, results revealed that most of samples exceeded the acceptable limits recommended by the WHO and ISIRI1053 standards for domestic and agricultural purposes. In most of the wells, groundwater was classified into saline and very hard categories. The analyses based on WQI values indicated that above 87% of water samples were unsuitable for drinking purposes. IWQ parameters expressed that 85%, 67%, 32%, 51%, 43% and 50% of samples had EC > 3000, Na% > 60%, MAR > 50%, KR > 1, SAR > 9 and Cl^- > 350, respectively, which were unsuitable for irrigation use. The dominant hydrochemical facies of water was Na–Cl–SO4 type, and 63% and 22.8% of samples were categorized as C4S4 and C4S3 class, with very high-salinity–high-sodium hazards and very high-salinity–high-sodium hazards, respectively. It indicated that most irrigated lands in this study area were affected by different levels of salinity and sodicity hazards that caused decreases in plant growth and crop productivity. The results can assist decision-makers and planners in prioritizing groundwater resources management in the region.

Keywords Physicochemical parameters · Groundwater quality · GIS-based maps · Drinking water standards · Irrigation water quality (IWQ)

Introduction

In arid and semiarid areas, groundwater is a vital resource for domestic, industrial and irrigation uses (Delgado et al. 2010, Yousefi et al. 2018). In these areas, over-exploitation of groundwater resources and successive long-term droughts in recent years caused decreases in groundwater levels and deterioration of groundwater quality by the accumulation of dissolved ions in water (Abbasnia et al. 2019, Chidambaram et al. 2022). Therefore, assessments of groundwater quality received more attention worldwide to provide safe water for various applications (Srinivas et al. 2013) and the hydrogeochemical behavior of groundwater was evaluated using various techniques such as binary plots, ionic ratios, Wilcox plots, Piper diagrams, Schoeller diagram, USSL diagrams and

✉ Reza Hassanzadeh
Hassanzadeh22@yahoo.com

Mohadeseh Hosseininia
m.hosseinyniya@yahoo.com

[1] Department of Water Engineering, Faculty of Water and Soil, Zabol University, Zabol, Iran

[2] Department of Ecology, Institute of Science and High Technology and Environmental Sciences, Graduate University of Advanced Technology, Kerman, Iran

GIS techniques (Chidambaram et al. 2022). Previous studies assessed water quality for irrigation and drinking purposes by considering major parameters such as electrical conductivity (EC), total dissolved solids (TDS), total hardness (TH), pH, SAR and major chemical elements, e.g., Ca^{2+}, Mg^{2+}, Cl^{-}, HCO_3^{-}, Na^{+}, K^{+} and SO_4^{2-} (Jamshidzadeh and Mirbagheri 2011, Pour et al. 2014, Alavi et al. 2016, Piroozfar et al. 2018, Abbasnia et al. 2019, Palmajumder et al. 2021, Rajmohan et al. 2021, Arota et al. 2022). Moreover, several studies applied GIS techniques, such as IDW and Kriging interpolation methods, in order to show the spatiotemporal variations of water quality that provide a better understanding of future water resources quality trends (Mosaferi et al. 2014, Alavi et al. 2016, Makki et al. 2021, Silva et al. 2021). Applying GIS in mapping of major parameters of groundwater quality has a significant impact on regional water management and future decision-making (Mohammadi et al. 2017, Chidambaram et al. 2022).

This study was conducted in Iran, Kavir Daranjir–Saghand basin, which is classified as one of the countries facing limited water resources due to its location in the arid and semiarid belt and lack of rainfall. Thus, the long-term rainfall statistics in the last 5 decades have shown a downward trend in annual precipitation to 243 mm (Mohammadjani and Yazdanian 2014). Kavir Daranjir–Saghand is a second-order watershed with an area of 50,737 km^2 in the central part of Iran. This basin is divided into 12 sub-basins including Rafsanjan, Kavir Daranjir, Kerman Baghin, Bafgh, Zarand, Arnan Dahaj, Bardsir, Bahadoran, Kohbanan, Gharyatolarab, Siriz Toghroljerd and Saghand. Rafsanjan plain is the biggest sub-basin in the Kavir Daranjir–Saghand basin and is located in the southwest part of this region. It is classified as a semiarid region, with 100 mm annual precipitation and mean annual potential evapotranspiration of 3000 mm (Hosseinifard and Mirzaei Aminiyan 2015). With population growth and the development of pistachio orchards in recent years, the high contribution of water needed by domestic, agricultural and industrial use highly depends on groundwater resources in the study area. Therefore, monitoring the quality of groundwater resources by water quality index (WQI) and standards (WHO and ISIRI1053), Schoeller diagram, irrigation water quality (IWQ) parameters, Piper, USSL and Wilcox diagram using GIS interpolation methods is the aim of conducting this study. The results can support groundwater resources management and its suitability for different consumptions in the coming years.

Materials and methods

Study area

Rafsanjan plain is the largest plain with an area of 12,513 Km^2 in the southwest part of the Kavir Daranjir–Saghand basin (covers about 25% of the basin), between longitude 290,000 to 470000E and latitude 331,000 to 3480000N in UTM projection system, and the area of the Rafsanjan aquifer is 4236 Sq. Km (Fig. 1a). The Rafsanjan plain consists of three main plains, namely Rafsanjan, Nough and Anar. The average height of the area is 1469 m above sea level. The high mountainous area is located in the west (Sarcheshmeh Mountains (Dehj–Sardoueye belt)) and east (Davaran Mountains) of this plain sloping down toward the central part of the plain (Fig. 1b).

The climate of the subjected area is semiarid, due to low annual rainfall (average 100 mm) and high annual potential evapotranspiration (average 3000 mm). Groundwater has been used for different purposes, such as domestic, agricultural and industrial usage in this area. In addition, irrigation of pistachio orchards is the main agricultural water use in this plain. There are 92,108 hectares of pistachio orchard and farmlands in the Rafsanjani plain (Fig. 1c) that uses 492 million cubic meters of groundwater per year.

Geological and hydrogeological profile of the aquifer

Surficial geological setting of the area composed of three main units: (1) alluvial and river deposits near the mountains in the southwest, west and northeast, (2) clay, salty and mud flat in the central part toward north and northwest, and (3) sand dunes covered mostly east and northeast part of the plain (Fig. 2 a). However, in the Rafsanjan plain, we are dealing with a complex setting of sedimentary and volcanic rocks as shown in Fig. 2b; the volcanic rocks are located in the south and south west of the study area (Sarcheshmeh Mountains (Dehj–Sardoueye belt)).

The aquifer geology and geohydrology consist of quaternary sediments that build an unconfined alluvial aquifer. Moreover, any compressed clayey layer that could be a potential for a confined aquifer has not been determined based on the analysis of geoelectric sounding profiles. The aquifer mainly consists of sand and clay and its thickness is around 100 m in the southwest and central parts of the plain. The aquifer thickness decreases toward the northwest of the plain due to the reduction in the depth of bedrock that causes shallow water table depth and creates salt marches and swamps in these part of the plain (Asar 2019). Furthermore, the evaluation of 128 geoelectric sounding profiles in this study area confirms the existence of salt water along fine-grained sediments in the northwest of this area (Anar region) and uplifted bedrock (Miocene gypsum and salt sediment) that caused shallow water table depth.

In the southeast part of the plain toward Sarcheshmeh Mountain, deep coarse-grained sediments that are suitable for composing the aquifer are identified. In the southeast toward the Kabootarkhan region, shallow sediments forming

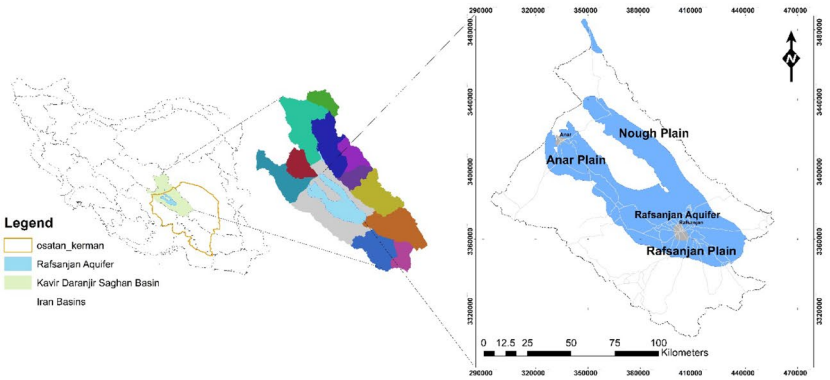

a. Study area: Rafsanjan plain, Rafsanjan Aquifer and Kavri Daranjir-Saghand basin in Iran

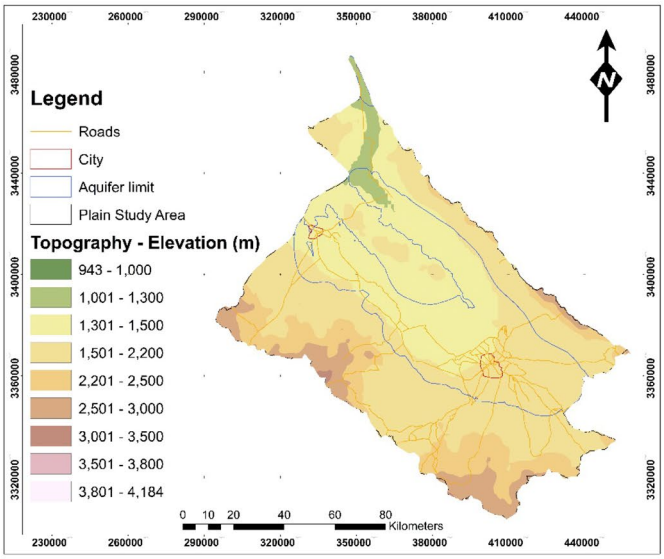

b. Topographic changes in Rafsanjan plain area

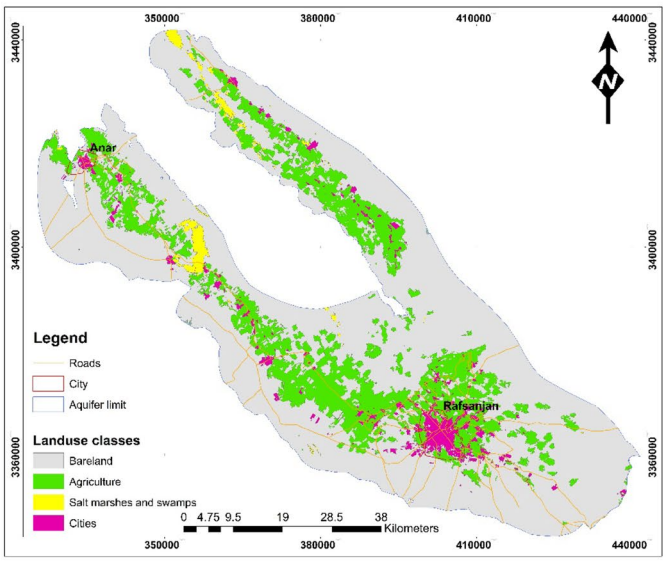

c. Land-use classes in Rafsanjan aquifier limit

Fig. 1 **a** Study area: Rafsanjan plain, Rafsanjan Aquifer and Kavir Daranjir–Saghand basin in Iran. **b** Topographic changes in Rafsanjan plain area. **c** Land-use classes in Rafsanjan aquifer limit

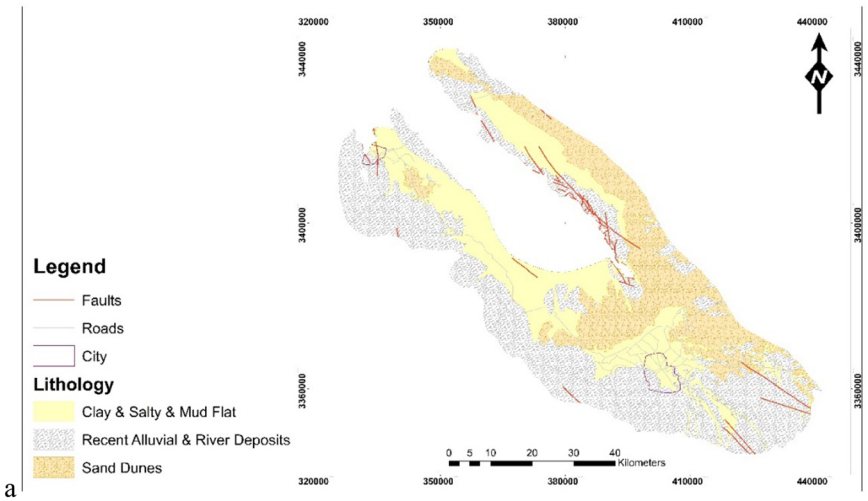

a

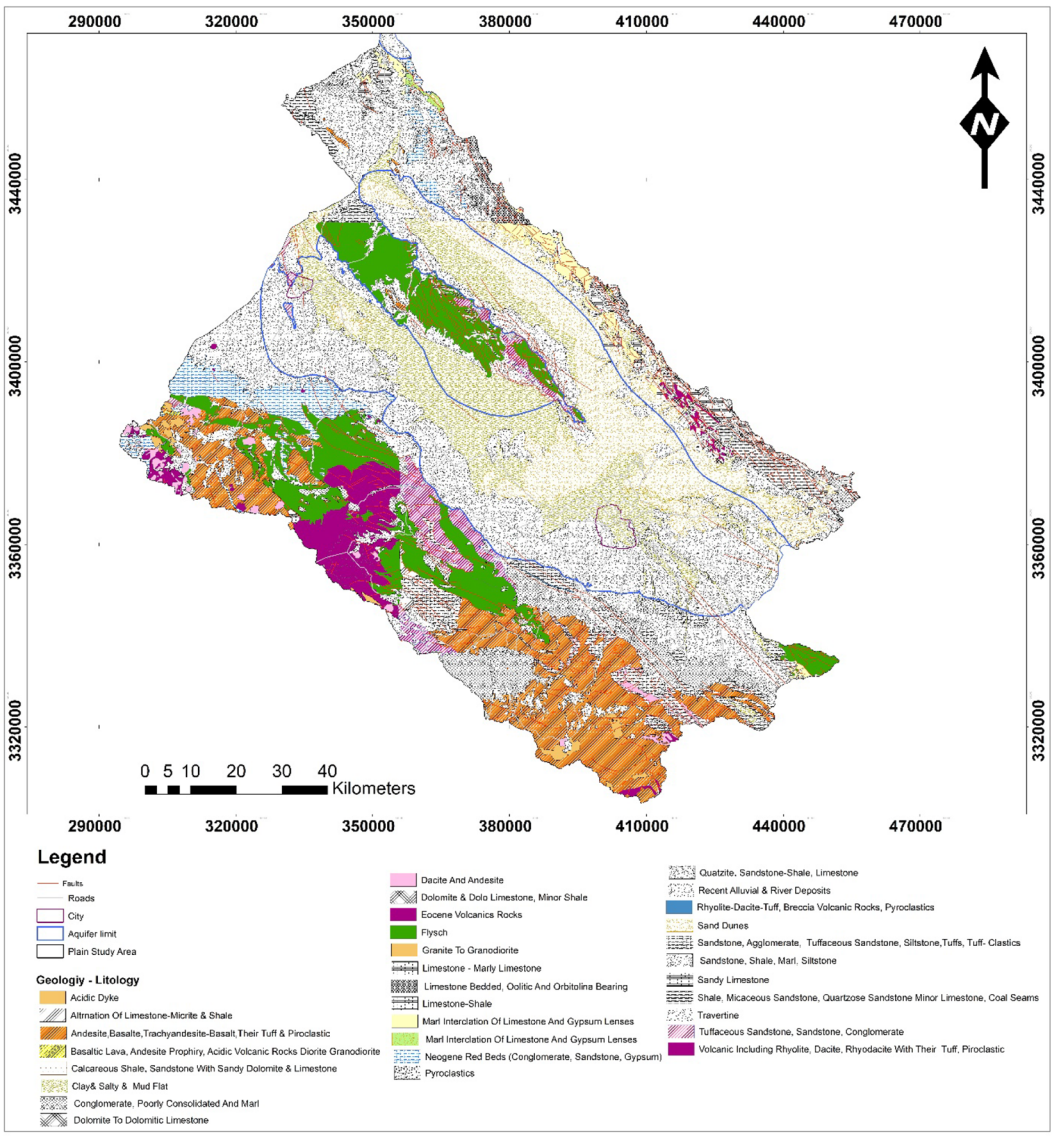

b

Fig. 2 **a** Geological setting of the Rafsanjan aquifer and **b** geological setting of the Rafsanjan plain

the aquifer and fine-grained sedimentary rocks of clay are distinguished. In the northeast toward the Nough region, limestone formation near the mountainous area and Oligomycin formation of gypsum and salt at this part of plain are spotted (Asar 2019).

The entrance of groundwater to the plain is located in the southeast from Kerman and Bardsir aquifer, and the groundwater flows from the southeast toward the northwest (Fig. 3a). The analyses of piezometric data (68 wells) indicate that the main recharge areas of the aquifer are located in the northeast and the southeast of the plain. The depth of groundwater ranges between 4.6 m and 177 m. This reaches 140 m in the margin of the plain and 60 to 40 m in the central parts, and then decreases to less than 20 m in the central parts toward the northwest of the plain (Fig. 3b).

The analysis of geological profiles of 7 exploration wells and 52 piezometric wells, which have been drilled in different years, shows the aquifer mainly consisting of gravel, silt, sand and clay in different depths and the amount of clay increases toward northeast part of the aquifer (Fig. 4 a to e).

Based on the analysis of sedimentological properties of logs of wells, a permeability map was produced. This map indicates very high to high permeability rates in the south, southwest and southeast of the plain due to the existence of coarse-grained sediment, and moderate to very low permeability rates in the north, northwest and northeast of the plain due to the existence of fine-grained sediment (Fig. 5).

Data gathering and analyses

In this study, the groundwater samples were collected from 55 different wells of Rafsanjan plain in the summer of 2020. Figure 2 shows the water sampling locations within the block. One-liter polyethylene bottles were used for sampling. Physicochemical parameters like pH and electrical conductivity (EC) of the water samples were taken by using pH meter and an EC meter, respectively. Total dissolved solids (TDS) were computed by multiplying the EC (μ Sm^{-1}) by a factor of 0.64. Table 1 reveals the standard laboratory procedures that were followed to determine the concentration of major ions (Pansu and Gautheyrou 2007).

The suitability of water for agricultural purposes was assessed by measuring parameters such as electrical conductivity (EC), sodium adsorption ratio (SAR), Kelly's ratio (KR), sodium percentage (Na%), residual sodium carbonate (RSC), magnesium absorption ratio (MAR) and permeability index (PI) (Table 2), and plotting the standard reference diagrams like Wilcox (1955), US Salinity Laboratory (USSL) (1954) and Piper (1944) diagrams.

The suitability of water for drinking purposes was determined by applying standard parameters such as World Health Organization (WHO 2011) and Institute of Standards and Industrial Research of Iran (ISIRI1053) (Water treatment physicochemical Specification of Iran (Tehran) 1997); the water quality index (WQI) and plotting the standard reference diagram such as Schoeller (Schoeller 1977).

In order to produce the spatial distribution of each element in the study area, inverse distance weighting (IDW) method was applied in GIS.

Results and Discussions

Variation of physicochemical parameters

Table 3 shows the flocculation of physicochemical parameters including pH, EC, TDS and TH, in Rafsanjan plain, where groundwater samples were collected.

Variations of pH

Figure 6a shows the contour plots for pH variation in summer 2020 in Rafsanjani plain. The pH values ranged from 5.8 to 8.1 with a mean of 7. The maximum value of pH was observed at the southwestern corner of the situ in Jafarabad Deighe (L 25), and the minimum pH value was situated at the northwestern region in Hojjatabad Anar (L 1). The decrease in pH results of the groundwater samples in the northwestern region of the basin (Anar plain) was caused by the sulfide volcanic rocks of the Sarcheshmeh Mountains (Dehj–Sardoueye belt), which is the main source of groundwater recharge in the Anar plain. Then, the water with low pH values was transferred to the end of the basin based on the flow gradient direction (Khajehpour and Abbasnejad, 2007; Malakootian & Khashi 2014). On the other hand, the presence of copper mines in the way of the groundwater slope toward the Anar plain caused a decrease in the pH values in the northwestern areas (Dehghan and Abbasnejad, 2011). The lowering pH of water and the high concentration of heavy elements of arsenic, lead and cadmium, which was affected by the sulfide veins of copper mines in this region, had also been reported in previous studies (Dehghan and Abbasnejad, 2011). Metal mines (such as gold, silver and copper) are often rich in sulfide minerals. The precipitation of sulfides exposed to weather leads to the formation of sulfuric acid. Sulfuric acid dissolves heavy metals and harmful metalloids (such as arsenic) from minerals and forms an acidic pH solution with high concentrations of arsenic, cadmium, lead, copper, etc. (Iatan, 2021). The research conducted by Honarmand et al., (2017) showed that the volcanic rocks of the Sarcheshmeh Mountains and the mineral processing of Sarcheshmeh copper factory led to a decrease in pH values an high amount of heavy elements in the water samples of the studied area (Honarmand et al. 2017). The effect of copper mine-induced pH decrease was also reported in Falun, central Sweden by Ek et al., 2001 (Ek

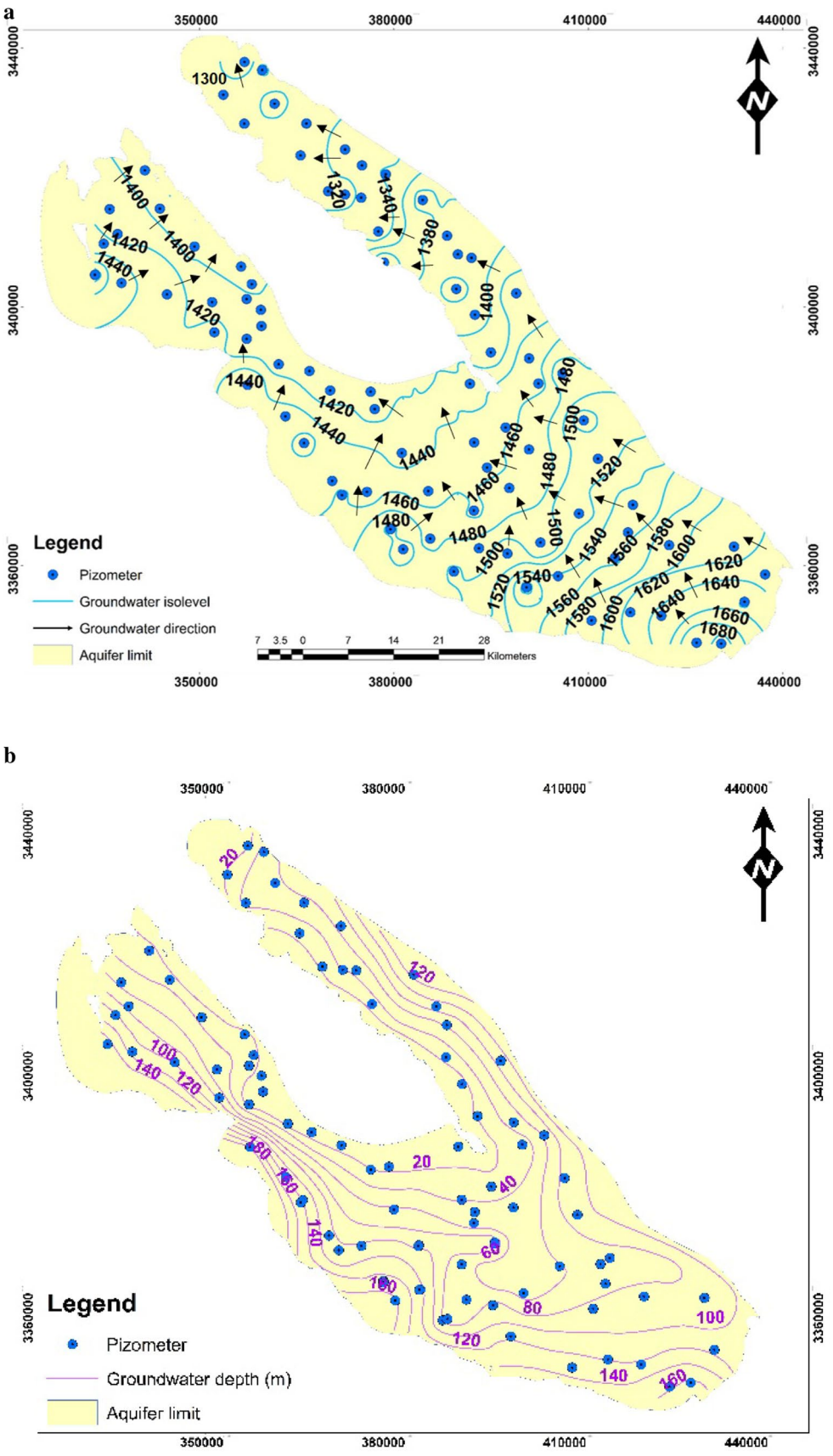

Fig. 3 **a** Groundwater flow direction and **b** groundwater depth in the study area

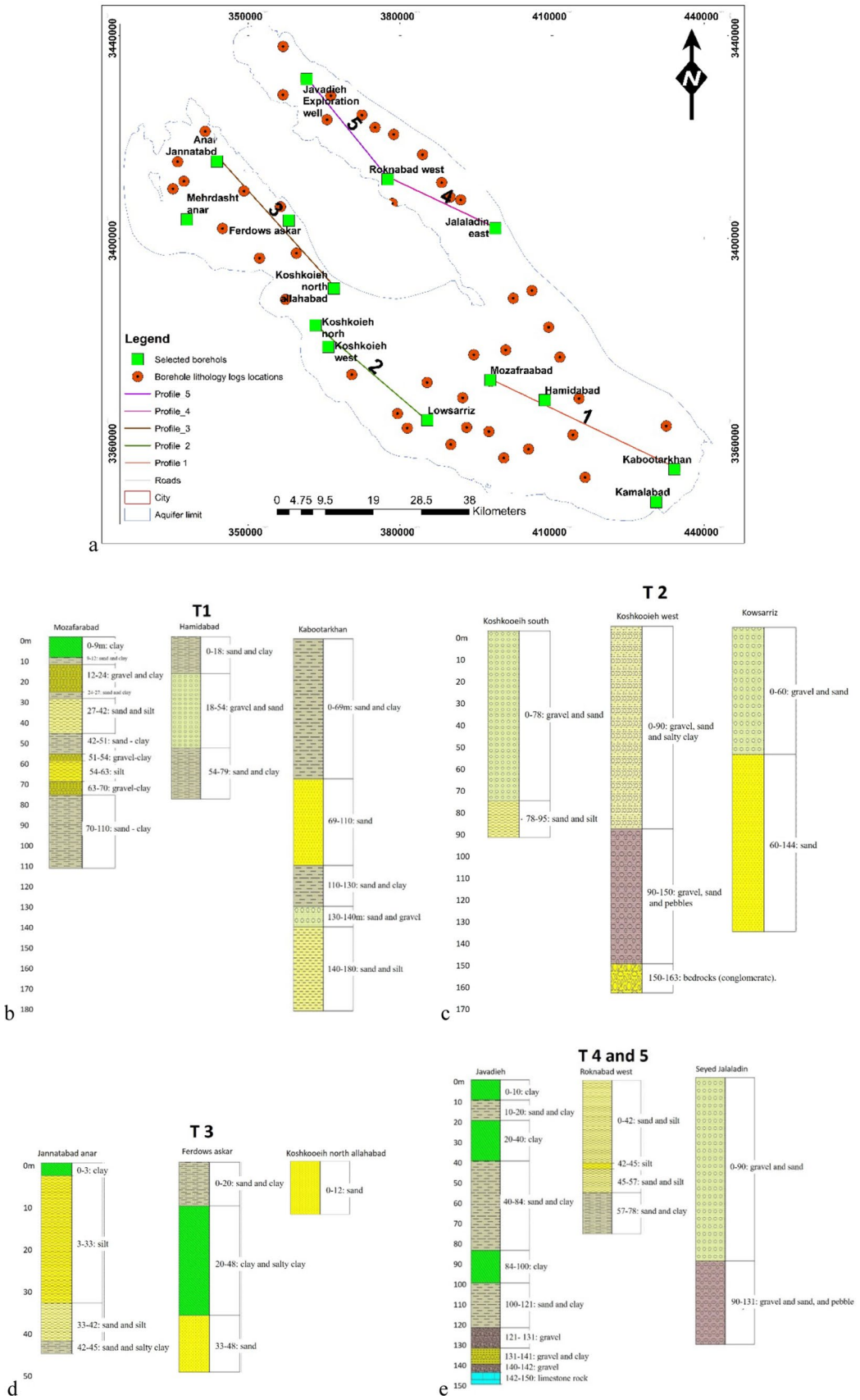

Fig. 4 **a** Location of selected boreholes in the study area, **b**–**e** geological logs of selected wells in the study area

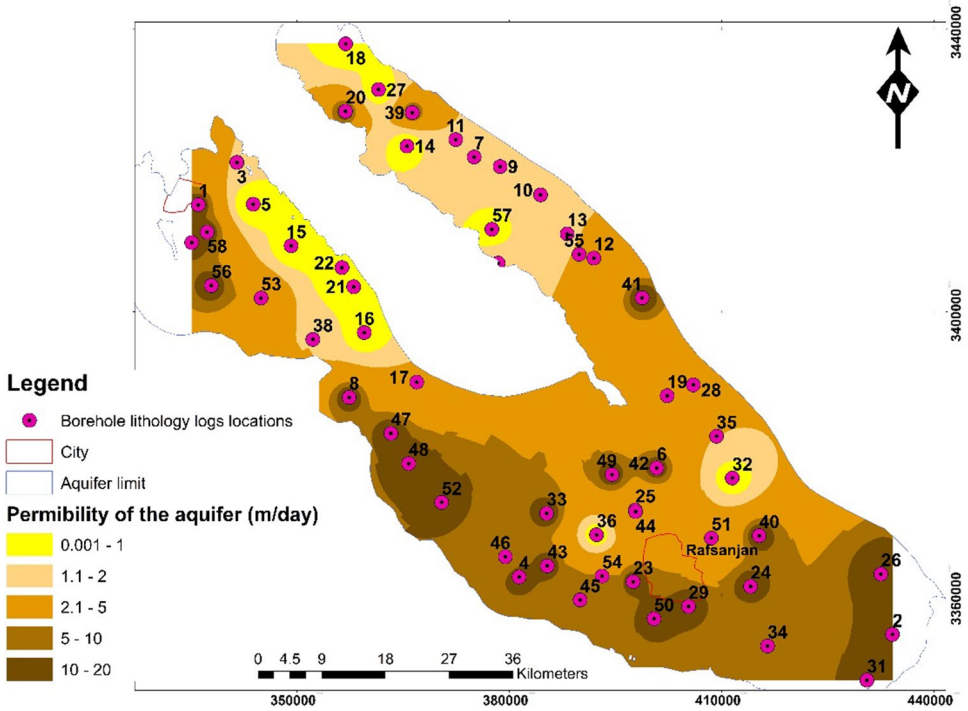

Fig. 5 Permeability of the aquifer in the study area

Table 1 Methods used to determine chemical parameters of water

Variables	Measuring tools
Ca^{2+}, Mg^{2+}	Titration method using standard EDTA
Cl^{-}	Titration method using standard $AgNO_3$
HCO^{-3}, CO^{-3}	Titration with HCl
Na^{+}	Flame photometry
SO_4^{-2}	Spectrophotometric turbidimeter

Table 2 Equation used to estimate the suitability for irrigation water quality (IWQ)

IWQ parameters	Reference
$SAR = \frac{Na^{+}}{\sqrt{(Ca^{2+}+Mg^{2+})}}$	Richards (1954)
$KR = Na^{+}/(Ca^{2+} + Mg^{2+})$	Kelly (1957)
$Na\% = \left\{ \frac{Na^{+}+K^{+}}{Na^{+}+K^{+}+Ca^{2+}+Mg^{2+}} \right\} * 100$	Wilcox (1955)
$RSC = (HCO_3^{-} + CO_3^{2-}) - (Ca^{2+} + Mg^{2+})$	Raghunath (1987)
$MAR = (Mg^{2+} * 100)/(Ca^{2+} + Mg^{2+})$	Paliwal (1972)
$PI = \frac{Na^{+}+\sqrt{HCO_3^{-}}}{Ca^{2+}+Mg^{2+}+Na^{+}} * 100$	Doneen (1964)

* Concentrations of all ions in the mentioned equations are in meq/L

& Renberg 2001). The research conducted by Sonon et al. (2007) showed that the presence of copper in groundwater samples of the Georgia region can lead to an increase in water acidity (Sonon et al. al., 2007).

The oxidation of dark Jurassic shales rich in pyrite in the recharge points of the Nough plain affected the groundwater pH and led to the acidity water. In the outlet of this region, the presence of sodium alkaline cations affected by the evaporative layers caused the pH levels to 7.6 (Hassanzadeh and Abbasnejad, 2019).

Variation of EC and TDS

The variation of EC and TDS is presented in the contour plots of Figs. 6b and 6c. The mean value of EC and TDS is 8041.4 µS/m and 5436.6 mg/l, respectively. Figure 6b and 6c clearly shows that the low values of EC and TDS were for the water of southeastern corner of the region and increased toward the northwestern zone. There was a close similarity of the variation of EC and TDS with the subsurface water flow from southeastern to northwestern zone in the situ. The maximum of EC and TDS was referred to Ishaqabad (L 7) in the northwestern zone, with the values of 29,300 µS/m and 19,045 mg/l, respectively.

According to Fig. 4 and Fig. 5, the soil texture changed from coarse-grained sediment in the south and southwest, to the fine-grained sediment in north and northwest; this caused different permeability rates and water movement in this plain. The decrease in the speed of water flow in the salt and swampy corridors toward the northwest area increased the concentration of soluble salts (Asar 2019). In the research conducted by Dehghan and Abbasnejad (2011), it was also reported that the main factor in high concentration of soluble salts of groundwater in the

Table 3 Names of locations and variations of physicochemical parameters in groundwater samples

Location number	Location name	pH	EC (µS/m)	TDS (mg/l)	TH (mg/l)
L 1	Hojjatabad Anar	5.8	6780	4407	2300
L 2	Anar	7.6	1433	931	200
L 3	Qasem Abad Anar	6	7300	4745	2080
L 4	Ali Abad Anar	6.5	12,140	7891	3600
L 5	Minodasht Anar	6.5	11,600	7540	3200
L 6	Ahmadabad Anar	6.2	18,160	11,804	5400
L 7	Ishaqabad	6.9	29,300	19,045	10,600
L 8	Aliabad Golshan Anar	6.6	21,700	14,105	10,000
L 9	Tawakul Abad Bayaz	6.8	26,400	17,160	6700
L 10	Rahmatabad Bayaz	7	14,900	9685	2200
L 11	Hemmatabad Sofla	7.2	10,500	6825	1700
L 12	Mohammadabad Sofla	6.8	15,600	10,140	4300
L 13	Javadieh Falah Falahie	6.7	10,000	6500	2800
L 14	Abbasabad Javadiyeh Fala	7.2	15,500	19,975	2700
L 15	Taghi Abad Kashkuyeh	7.5	8770	5701	1300
L 16	Mohammadabad Nogh	7	9550	6208	2000
L 17	Bahmanabad	7.5	10,600	6890	1600
L 18	Ali Abad Fallah	6.9	8780	5707	1300
L 19	Bahmanabad Koshkuyeh	7.4	8940	5811	1000
L 20	Sadrabad Nogh	7	9350	6078	1700
L 21	Javadieh Fallah—Roy Qan	7	4150	2698	750
L 22	Ali Abad Haj Sheikh Ali	7.2	6000	3900	1000
L 23	Ahmadiyya Nogh	7	5100	3315	840
L 24	Islamabad Nogh	6.9	7500	6500	1300
L 25	Jafarabad Deighe	8.1	1160	754	70
L 26	Golazar Koshkuyeh	7.1	5700	3705	800
L 27	Sadrabad Nogh	7	10,100	6565	2400
L 28	Jalilabad Nogh	7	6000	3900	1200
L 29	Segharyeh Jahrom	7.4	3660	2379	650
L 30	Rokan Abad Nogh	7	9300	6045	3000
L 31	Akbarabad Arab	7.4	7660	4979	1000
L 32	Manzarieh	7	6000	3900	1100
L 33	Asadabad Bahrman	6.3	8800	5720	1500
L 34	Ferdowsi Nogh	7.2	10,800	7020	2200
L 35	Qaderabad Nogh	7.3	4000	2600	700
L 36	Wakil Abaddianti	6.8	5850	3803	1800
L 37	Mohammadabad Koshkuyeh	7.2	8400	5460	1800
L 38	Najaf Abad	7.2	6600	4290	1200
L 39	Tavakol Abad Nogh	7.3	9000	5850	1900
L 40	Hussein Abad Ismaili	6.5	4880	3172	1300
L 41	Hassanabad Goldasht	6.9	3950	2568	500
L 42	Abbasabad Nogh	6	8290	5389	2100
L 43	Enayat Abad Nogh	7.4	4800	3120	1200
L 44	Zarrin Dasht	6.4	6100	3965	1500
L 45	Roie Ghanat Ahmadabad	7.4	4640	3016	1000
L 46	Ghanat Dehshikh	6.9	695	452	120
L 47	Tajabad	7.8	2850	1853	320
L 48	Akbar Abadjari	7.3	3930	2555	900
L 49	Mehdi Abad Vahed	7	2860	1859	330
L 50	Saeed Abad	7.9	850	553	100
L 51	Goldasht Davaran	6.9	3850	2503	700

Table 3 (continued)

Location number	Location name	pH	EC (µS/m)	TDS (mg/l)	TH (mg/l)
L 52	Jannat Asadi	7.5	4000	2600	1000
L 53	Nasiriyah Brothers	7.4	2670	1736	200
L 54	Istgah Keshavarzi Naser	7.2	1580	1027	370
L 55	Aliabad Kabutarkhan	7.2	3250	2113	575
Mean		7.0	8041.4	5436.6	1892.8
Maximum		8.1	29,300	19,975	10,600
Minimum		5.8	695	452	70

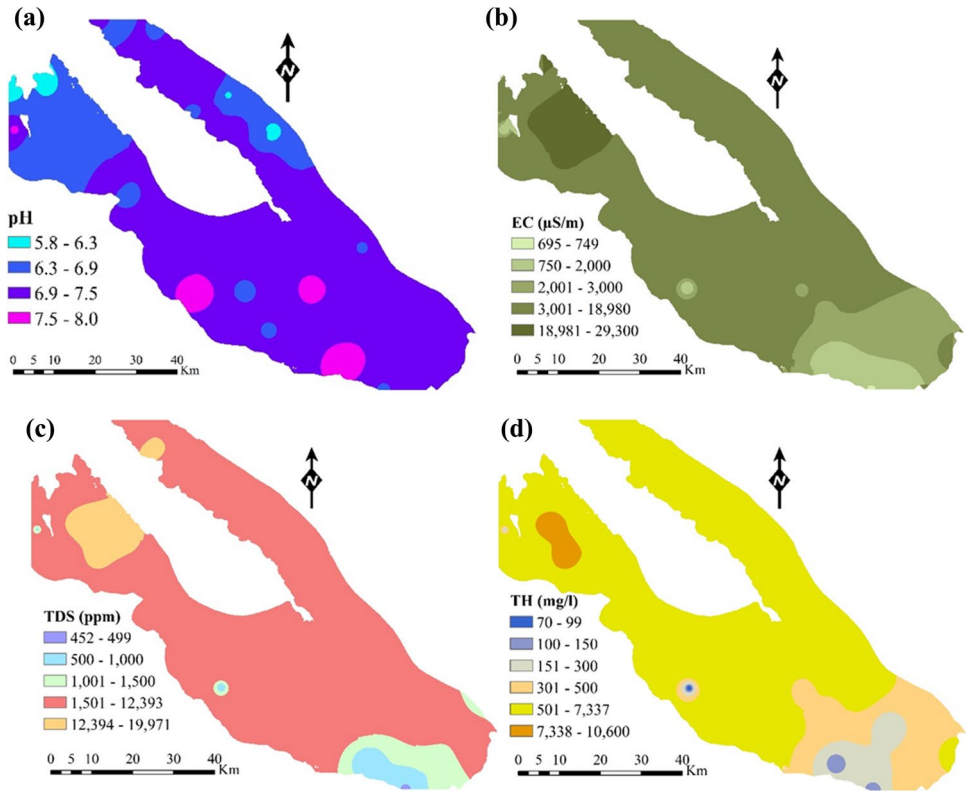

Fig. 6 Spatial distribution of **a** pH; **b** electrical conductivity (EC); **c** total dissolved solids (TDS) and **d** total hardness (TH) in Rafsanjan plain

northwestern parts of Rafsanjan plain was the groundwater flow in contact with bedrock containing gypsum and salt deposits (Upper Red Formation) (Dehghan and Abbasnejad, 2011). Therefore, based on the groundwater flow from the southeast parts (with lighter soil textures and higher permeability) to the northwest corner (fine soil texture with gypsum and salt deposits layers) the dissolution rate and the TDS values increased. In the research of Mirnezami et al. (2018), it was reported that the geological features in the northwestern parts of Rafsanjan plain had caused the water of many wells unusable for agricultural purposes due to excessive salts (Mirnezami et al. 2018). On the other hand, the increase in the number of authorized and unauthorized wells and over-exploitation in the northwestern part of the plain had led to an increase in electrical conductivity (EC) (Salehi et al. 2022). The over-exploitation of groundwater in areas with limestone and salt deposit layers (such as pistachio farming areas in Anar plain) had a significant effect on decreasing water quality (Rahnama and Zamzam 2013, Mirnezami et al., 2018).

In the northwest of the aquifer toward the Nough plain, the presence of shallow sediments of fine-grained and clay sedimentary rocks had also reduced the water flow. The low water flow through the limestone formation, gypsum and salt deposit layers caused the dissolution of more salts and the high TDS values (Hassanzadeh and Abbasnejad, 2019). Therefore, the different geological and hydrogeological attributes led to a significant difference in the EC and TDS values in the various parts of Rafsanjan plain.

Variation of TH

Figure 6d shows the contour plot of total hardness (TH) of the study area. The TH varied from 70 mg/l in Jafarabad Deighe (L 25) to 10,600 mg/l in Ishaqabad (L 7), with an average of 1892.82 mg/l. From the maps, it is clear that for the entire studied area the low values of TH were for the water samples of the southeastern corner of the region and exceeded rapidly toward the northwestern zone. Like EC and TDS, the TH variations were on the same pattern of groundwater flow and were affected by the evaporative deposition subsurface layers.

Variation of major ions

Table 4 presents the concentration and variation of major cations and anions like calcium (Ca^{2+}), magnesium (Mg^{2+}), sodium (Na^{+}) and chlorine (Cl^{-}), sulfate ($SO_4{}^{-2}$) and bicarbonate ($HCO_3{}^{-}$), respectively. The maximum concentration of major cations was plotted for the northwestern areas of the plain (Figs. 7a, 4b, 4c), with 2200 (mg/l) for calcium in Aliabad Golshan Anar (L 8) 1296 (mg/l) for magnesium in Ishaqabad (L 7) and 5520 for sodium in Ishaqabad (L 7). The mean concentrations of major cation were 380.3, 226.1 and 1434.9 mg/l for calcium, magnesium and sodium, respectively. The highest value of anions, i.e., chlorine, was observed at the northwestern of the area (Fig. 7e). However, the maximum concentrations of two other anions were reported 1159 mg/l at Zarrin Dasht (L 44) and 3456 mg/l at Abbasabad Javadiyeh Fala (L 14) for bicarbonate and sulfate, respectively.

The previous research showed that concentration of cations and anions had a high correlation with the EC and TDS values (Hosseinifard et al., 2015; Aminiyan et al. 2016). Therefore, based on the results in "Variation of EC and TDS" part, the high concentration of ions in the northwestern areas (Anar plain) was strongly affected by the geological and hydrogeological features, i.e., fine soil texture, low permeability and water flow through gypsum layers and salt deposits. The reason for high concentration of ions in the Nough plain had explained by the previous research. Hassanzadeh and Abbasnejad (2019) reported that the low-speed water flow through the evaporative sediments caused an increase in the dissolution of soluble salts, especially chlorine and sodium concentration, in the northwestern areas of Nough plain (Hassanzadeh and Abbasnejad, 2019).

Assessment of water quality for domestic use

Drinking water standards

The physicochemical parameters of groundwater samples had been compared with drinking water standard that recommended by the WHO (WHO 2011) and ISIRI1053 (Water treatment physicochemical Specification of Iran (Tehran) 1997) for safe drinking usages. The ranges of pH values in groundwater samples, with mean value of 7.02, indicated that all samples were within acceptable limits (Table 5). The EC values of all the groundwater samples were considerably higher than the acceptable limits in comparison with both drinking water standards (Fig. 8). Another significant factor for assessing the suitability of drinking water is total dissolved solids (TDS). According to WHO and ISIRI1053, TDS values were higher than 1500 mg/L resulted in an unpleasant taste. As, 50 samples were above acceptable limit (about 88%—Fig. 8) while only 5 samples were categorized in suitable class for drinking purposes (Table 5). Based on Sawyer and McCartly (1967), the total hardness (TH) of groundwater samples is classified into four classes: soft (75 mg/L), moderately hard (75–150), hard (150–300) and extremely hard (> 300). Accordingly, about 2%, 3%, 7% and 88% of the groundwater samples in the present study area were classified as soft, moderately hard, hard and very hard, respectively.

The suitability of water is generally evaluated by the concentration of major ions. Table 5 presents the comparison analysis for the concentration of major cations and anions in water samples and the drinking water standards acceptable limits. However, among all reported ions, the sodium and chlorine concentrations in most of water samples are at the critical limit and of serious concern for drinking purpose. They may be due to the source of the evaporative deposition layer in the present study area (Fig. 8).

Water quality index

The water quality index (WQI) is an effective tool for assessing the suitability of groundwater for drinking purposes. In addition, it is a worldwide method to evaluate the impact of human activities on natural groundwater quality (Vasanthavigar et al. 2010, Logeshkumaran et al. 2015). The calculation of the WQI was done by considering weights that range from 1 to 5 for each parameters, based on its relative importance (Logeshkumaran et al. 2015). Table 6 presents the WQI weights and relative weight of physiochemical parameters. According to Arota et al. (2022), the WQI is calculated in four steps (Eqs. 1–4):

$$Wi = \frac{wi}{\sum_{i=1}^{n} wi} \quad (1)$$

where *W*i is the relative weight, wi is the weight of each parameter and n is the number of parameters. In the second step, the quality rating scale for each parameter is calculated by dividing its concentration in each water sample by

Table 4 Concentration of major cation and anions in groundwater samples

Location number	Ca^{2+} (mg/l)	Mg^{2+} (mg/l)	Na^{+} (mg/l)	HCO_3^{-} (mg/l)	CL^{-} (mg/l)	SO_4^{2-} (mg/l)
L 1	520	240	598	640.5	1775	552
L 2	60	12	262.2	427	213	115.2
L 3	460	223.2	920	976	2272	76.8
L 4	760	408	1656	378.2	3550	1814.4
L 5	720	336	2093	244	4047	1776
L 6	1200	576	2990	317.2	7100	1574.4
L 7	2080	1296	5520	152.5	13,845	2856
L 8	2200	1080	1932	152.5	7455	3432
L 9	1440	744	5175	91.5	11,360	1800
L 10	480	240	3910	183	5325	2928
L 11	440	144	2530	85.4	3692	1852.8
L 12	680	624	3105	122	5822	2640
L 13	640	288	1771	97.6	3550	1507.2
L 14	480	360	3680	122	4970	3456
L 15	340	108	1840	85.4	2840	1180.8
L 16	360	264	1909	122	3195	1488
L 17	400	144	2530	61	3905	1488
L 18	240	168	1610	213.5	2840	600
L 19	180	132	1978	109.8	2698	1353.6
L 20	240	264	1656	134.2	2982	950.4
L 21	140	96	655.5	341.6	994	475.2
L 22	220	108	1035	91.5	1846	552
L 23	180	93.6	966	463.6	1349	633.6
L 24	240	168	1265	134.2	2414	518.4
L 25	16	7.2	250.7	244	195.25	134.4
L 26	120	120	1104	158.6	1704	643.2
L 27	440	312	1656	97.6	3763	595.2
L 28	200	168	1039.6	402.6	1562	892.8
L 29	100	96	618.7	390.4	781	552
L 30	500	420	1380	183	2982	1584
L 31	240	96	1426	207.4	1988	1084.8
L 32	260	108	1035	146.4	1775	700.8
L 33	160	264	1610	1098	2307.5	816
L 34	360	312	2070	109.8	3976	969.6
L 35	140	84	690	244	994	576
L 36	360	216	671.6	122	1704	729.6
L 37	360	216	1495	622.2	2343	1190.4
L 38	260	132	1173	73.2	1988	854.4
L 39	400	216	1656	73.2	3124	998.4
L 40	280	144	690	671	1278	432
L 41	140	36	738.3	97.6	1136	408
L 42	320	312	1173	1134.6	2272	499.2
L 43	200	168	694.6	158.6	1278	748.8
L 44	280	192	959.1	1159	1420	609.6
L 45	160	144	736	122	1420	480
L 46	40	4.8	115	244	78.1	57.6
L 47	20	64.8	402.5	91.5	532.5	355.2
L 48	180	108	581.9	122	994	638.4
L 49	90	25.2	584.2	91.5	355	984
L 50	20	12	156.4	219.6	92.3	124.8

Table 4 (continued)

Location number	Ca^{2+} (mg/l)	Mg^{2+} (mg/l)	Na^{+} (mg/l)	HCO_3^{-} (mg/l)	CL^{-} (mg/l)	SO_4^{2-} (mg/l)
L 51	160	72	671.6	152.5	994	609.6
L 52	200	120	637.1	73.2	1278	504
L 53	40	24	531.3	457.5	497	268.8
L 54	60	52.8	241.5	378.2	266.25	201.6
L 55	110	72	542.8	146.4	745.5	561.6
Mean	380.3	226.1	1434.9	277.1	2652.0	1007.7
Maximum	2200	1296	5520	1159	13,845	3456
Minimum	16	4.8	115	61	78.1	57.6

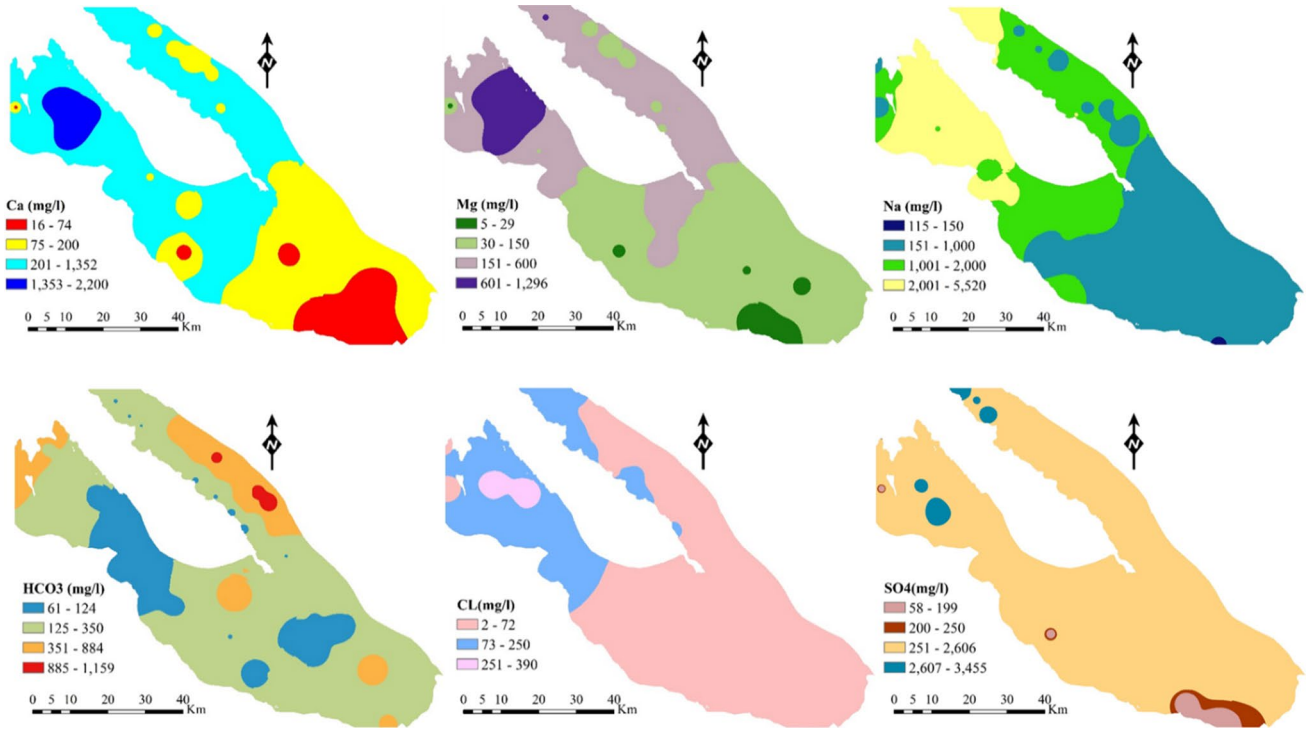

Fig. 7 Spatial distribution of major cations and anions in the study area

its respective standards (WHO 2011) and multiplying the results by 100 (Eq. 2):

$$qi = \left(\frac{Ci}{Si}\right) * 100 \tag{2}$$

where qi is the quality rating, Ci is the concentration of each parameter in each groundwater sample in (mg/L) and Si is the (WHO 2011) standard for each parameter in mg/L. In the third step, the subindex (SIi) is determined for each parameter (Eq. 3). Therefore, in the final step the sum of SI values gives the water quality index for each groundwater sample (Eq. 4):

$$SIi = Wi * qi \tag{3}$$

$$WQI = \sum SIi \tag{4}$$

where SIi is the subindex of ith parameter, Wi is the relative weight, Qi is the rating based on the concentration of ith parameter and WQI is the water quality index of each sample.

Drinking water quality is classified into five classes as excellent, good, poor, very poor water quality and unsuitable for drinking, based on WQI values (Palmajumder et al.

Table 5 Measured ranges of physicochemical parameters of groundwater and comparison with drinking water standards

Measured parameters	Measured range	Mean	WHO		ISIRI1053	
			Acceptable limits [1, 2]	No. of samples above acceptable limits	Acceptable limits	No. of samples above acceptable limits
pH	5.8 8.1	7.02	6.9 9.2	0	6.5–8.8	0
EC (µS/cm)	695 29,300	8041.4	300	55	300	55
TDS (ppm)	452 19,975	5436.58	500 1500	50	1500	50
TH (mgl^{-1})	70 10,600	1892.82	10 500	46	500	46
Ca^{2+} (mgl^{-1})	16 2200	380.3	75 200	32	300	23
Mg^{2+} (mgl^{-1})	4.8 1296	226.1	30 150	27	30	49
Na^{+} (mgl^{-1})	115 5520	1434.9	50 60	55	200	53
HCO_3^{-} (mgl^{-1})	61 1159	277.1	125 350	14	–	–
SO_4^{2-} (mgl^{-1})	57.6 3456	1007.7	200 250	49	250–400	47
Cl^{-} (mgl^{-1})	78.1 13,845	2652.0	250	51	250–400	49

TDS: Total dissolved solids; *EC*: electrical conductivity; *TH*: total hardness; *WHO*: World Health Organization; *ISIRI1053*: Institute of Standards and Industrial Research of Iran, Drinking water

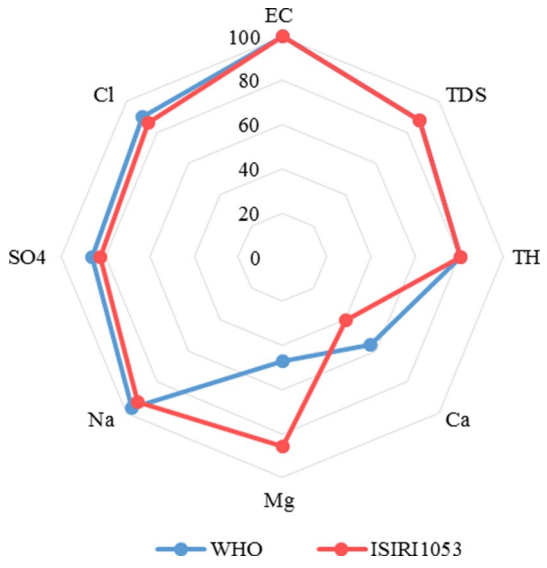

Fig. 8 Percentage of physicochemical parameters above the permissible limit for WHO and ISIRI1053 standards

2021). In the Rafsanjan plain, none of samples was classified in the excellent class and only few samples in good quality class (Table 7). 3.6% of the samples were classified as poor water quality based on two standards, and 1.8% and 3.6% of the samples were categorized in very poor water quality class according to WHO and ISIRI1053 standards, respectively. The rest of the samples were classified as unsuitable for drinking (WQI > 100) category, with 92.7% and 87.3% for WHO and ISIRI1053 standards, respectively (Table 7).

Figure 9 shows the spatial distribution of the WQI for both standards. The samples with poor and very poor water quality were situated in the southeast and some parts of the west and northwest of the region (Fig. 9).

Schoeller diagram

Schoeller diagram (1977) is the most popular method to classify the suitability of drinking water quality (Alavi et al. 2016, Almodaresi et al. 2019, Panahi et al. 2021). The diagram is based on the concentration of major cations (Ca^{2+}, Mg^{2+}, Na^{+}), anions (Cl^{-}, HCO^{3-}, SO_4^{2+}), total dissolved solids (TDS) and total hardness (TH). According to this diagram, the quality of drinking water is classified into six zones including good, acceptable, inappropriate, bad, temporarily drinkable in emergency and undrinkable (Choramin, Safaei et al. 2015). Figure 10 shows that most of the water samples fell in the limits of 'bad' and 'temporarily drinkable in emergency' zones. Water samples with good quality were located in the southeast corner of the region and

Table 6 Assigned weight and relative weight of physiochemical parameters in water quality index

Parameters	WHO standard	Iranian standard	Weight (wi)	Relative weight (Wi)
TDS (ppm)	500–1500	1500	5	0.179
Ca^{2+} (mgl^{-1})	75–200	300	2	0.071
Mg^{2+} (mgl^{-1})	30–150	30	1	0.036
Na^{+} (mgl^{-1})	50–60	200	2	0.071
HCO_3^{-} (mgl^{-1})	125–350	–	3	0.107
SO_4^{2-} (mgl^{-1})	200–250	250–400	4	0.143
Cl^{-} (mgl^{-1})	250	250–400	3	0.107

Table 7 Water quality classification based on WQI value for WHO and ISIRI1053 standards

WQI value	Rating of water quality	WHO standard		ISIRI1053 standard	
		Number of samples	Percentage of the water samples	Number of samples	Percentage of the water samples
0–25	Excellent water quality	0	00	0	00
26–50	Good water quality	1	1.8%	3	5.5%
51–75	Poor water quality	2	3.6%	2	3.6%
76–100	Very poor water quality	1	1.8%	2	3.6%
Above 100	Unsuitable for drinking	51	92.7%	48	87.3%

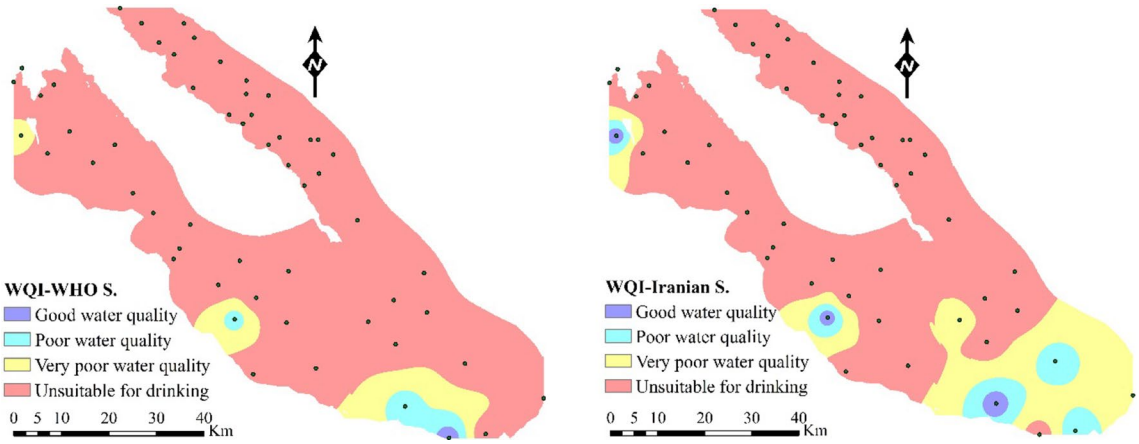

Fig. 9 Spatial distribution of water quality index (WQI) for two standards (WHO and ISIRI1053) in the study area

declined toward the central to northwestern zone as shown in Fig. 10b. Among 55 water samples, about 2%, 5%, 7%, 33%, 40% and 13% of the samples fell under good, acceptable, inappropriate, bad, temporarily drinkable in emergency and undrinkable categories for drinking purposes, respectively (Fig. 10c).

Assessment of water quality for agriculture

The suitability of water for agriculture purposes has been investigated by different studies (Choramin et al. 2015, Palmajumder et al. 2021, Arota et al. 2022, Singh et al. 2022). EC, SAR, Na%, MAR, KR, RSC, PI and Cl^{-} were the most popular parameters to evaluate the suitability of groundwater quality for irrigation usage (Tripathi et al. 2012). Table 8 reveals the classification of groundwater samples according to these parameters. In addition, a graphical representation of the suitability of water samples for irrigation purposes was plotted based on the US salinity, Wilcox and Piper diagrams.

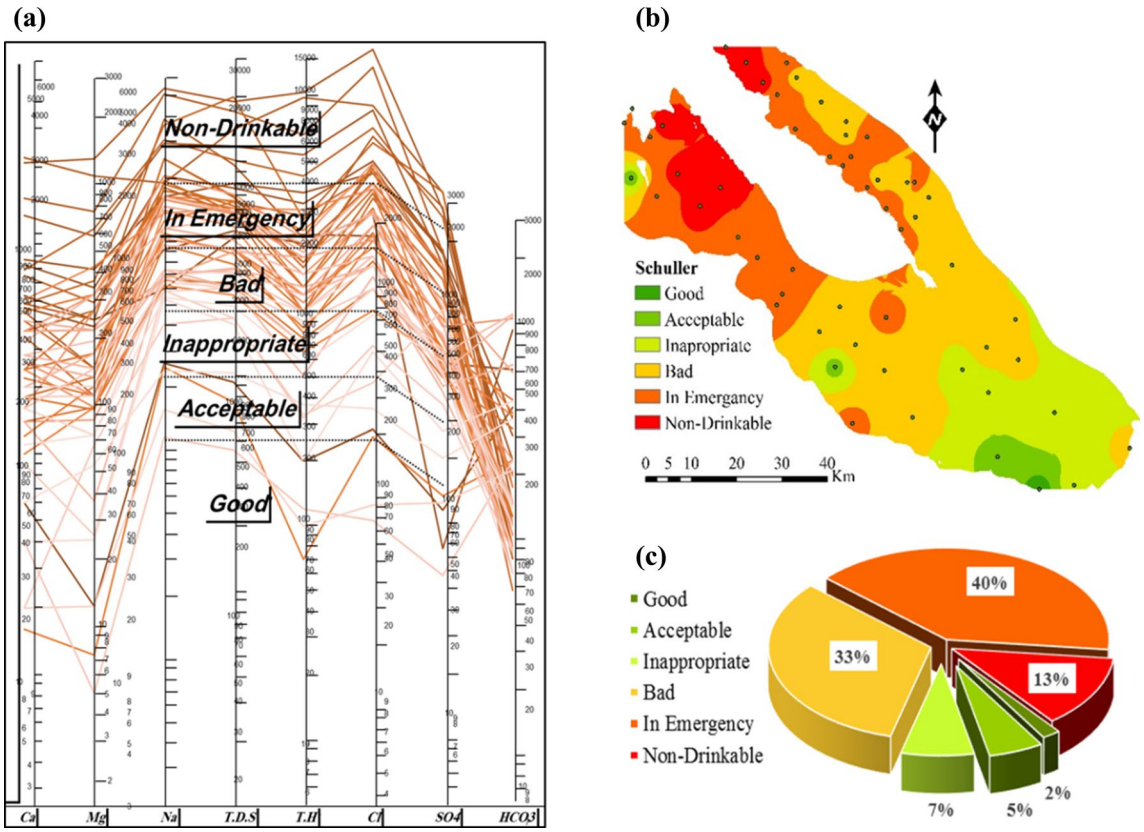

Fig. 10 **a** Schoeller diagram of 55 drinking water samples and **b** spatial distribution of its categories; c) percentage of the samples in each category in the studied area

Salinity hazard (EC)

Irrigation with saline water was identified as the primary factor reducing plant growth and crop production (Baghalian, Haghiry et al. 2008). Electrical conductivity (EC) is an important factor for classifying the salinity hazard and the suitability of irrigation water. According to Wilcox (1955), the salinity of irrigation water was classified into five classes based on EC values (Table 8). Analyses of water samples showed that one groundwater sample was under good class, and 4 and 3 samples were in the permissible and doubtful class, respectively. 85% ($n=47$) of groundwater samples fell under the unsuitable class, which covered most parts of studied area (Table 8). These results showing samples with low salinity levels were located in the east corner of the plain, and it increases from the center toward the northwest of the Rafsanjan plain.

Sodium absorption ratio (SAR)

In Table 8, the alkalinity hazard of irrigation water was defined by SAR parameter. Following these classifications, about 25% and 49% of groundwater samples were under excellent and good classes that were situated in the east and southeast parts. The alkalinity hazard increased, i.e., permissible (15% of the samples) and doubtful (11% of the samples) categories, toward the northwest. Since SAR reflects the effect of sodium relative to calcium and magnesium, high concentrations of sodium in the central and northeast areas related to the existence of evaporative deposition layers in this area.

Sodium percentage (Na%)

The high sodium content destroys the soil structure, decreases soil permeability and damages crop production (Prihar et al. 1985). Thus, it is introduced as essential parameter to assess irrigation quality (Singh et al. 2022). The sodium percentage (Na%) of collected samples was classified into five categories recommended by Wilcox (1955) guideline. Table 8 shows most of groundwater samples were under permissible (16%) and doubtful (34%) classes.

Magnesium adsorption ratio (MAR)

According to Paliwal (1972), MAR is classified into two classes, i.e., MAR > 50% are suitable and MAR < 50% are unsuitable for agricultural purposes. Based on this category,

Table 8 Classification of groundwater samples based on irrigation water quality (IWQ) parameters

IWQ parameters		Range	Class	Number of samples	Maps	Graph
EC (µS/cm)		< 250	Excellent	0	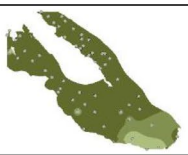	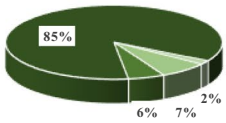
		250–750	Good	1		
		750–2000	Permissible	4		
		2000–3000	Doubtful	3		
		> 3000	Unsuitable	47		
SAR		< 10	Excellent	14		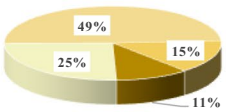
		10–18	Good	27		
		18–26	Permissible	8		
		> 26	Doubtful	6		
Na%		< 20	Excellent	0		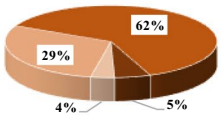
		20–40	Good	2		
		40–60	Permissible	16		
		60–80	Doubtful	34		
		> 80	Unsuitable	3		
MAR		> 50 %	Suitable	25	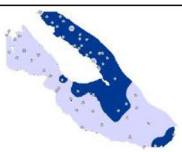	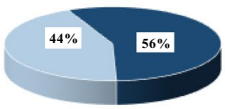
		< 50%	Unsuitable	32		
KR		< 1	Suitable	4		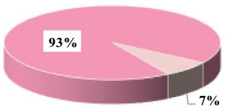
		> 1	Unsuitable	51		
RSC		< 0.5	Low	50	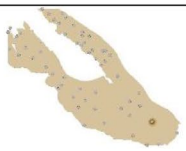	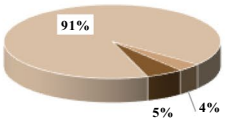
		1.25–2.50	Medium	2		
		> 2.50	High	3		
PI		> 75%	Good	17		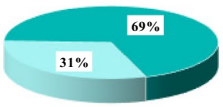
		25-75%	Suitable	38		
		< 25%	Unsuitable	0		
Specificion toxicity	Na^+ (SAR)	< 3	None	0		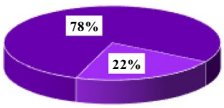
		3–9	Moderate	12		
		>9	Severe	43		
	Cl^- (mg/l)	< 140	None	2	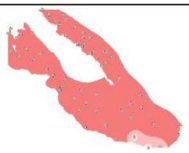	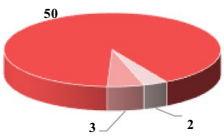
		140–350	Moderate	3		
		> 350	Severe	50		

it can be concluded that about 56% (n = 32) were not suitable and safe for irrigation, as shown in Table 8.

Kelly's ratio (KR)

In 1957, Kelly represented a parameter that KR value < 1 meant suitable irrigation water, while those values greater than this ratio were considered unsuitable (Kelly 1957). Thus, out of 55 water samples in the present studied area, about 93% of samples were unsuitable for irrigation use (Table 8).

Residual sodium carbonate (RSC)

The residual sodium carbonate is a parameter to evaluate the ability of irrigation water to reduce free calcium and magnesium in the soil (Sagar 2015). The RSC value < 0 indicates a little risk of sodium accumulation due to offsetting levels of calcium and magnesium, while positive values indicate sodium accumulation in the soil due to trapping free calcium and magnesium by the bicarbonate and carbonate (Raju 2007). Based on concluded samples in the studied area, except in five locations, about 91% ($n = 50$) of the groundwater samples had negative RSC value with a low risk of sodium accumulation (Table 8). The RSC geospatial map shows that the application of the groundwater for irrigation use has little impact on the deposition of free calcium and magnesium in almost all locations (Table 8).

Permeability Index (PI)

The long-term effect of irrigation water usage with high levels of Na^+ and HCO_3^- on soil permeability has been evaluated by Doneen (1964). In this region, PI varies from 30 to 98 with a mean value of 67 ± 12. Table 8 shows that 31% and 69% of samples come under good to suitable categories for irrigation, respectively. The good quality water samples were situated in the southwest and western areas, while the other parts of the studied area fell under the suitable class (Table 8).

Specific ion toxicity

The cause of toxicity problems in plants is high concentrations of certain ions, such as sodium and chloride, in water or soil. According to plant type and sensitivity, the significant uptake and accumulation of these ions in the plants lead to crop damage or yield reduction (Simsek and Gunduz 2007). However, the sensitivity of the permanent crops to this type of toxicity is more than the annual crops (Ayers and Westcot 1985). Therefore, since Rafsanjan plain is Iranian's foremost producer of pistachio, the evaluation of ion toxicity in water for irrigation purposes is essential.

Sodium

As sodium affects soil physical properties and plant survival, the assessment of sodium hazard is expressed separately. Table 8 presents the classification of irrigation water quality based on its SAR value, which generally defines as sodium hazard. Except for some regions in the east and southeast ($n = 12$), about 78% of water samples were under severe sodium conditions and were unsuitable for irrigation use and causing more problems such as the appearance of toxicity symptoms on the plant, damage to crop quality and productivity, and reduced permeability and water infiltration (Ayers and Westcot 1985, Flowers, Munns et al. 2015).

Chloride

Chloride is another ion that, at high levels, can cause toxicity problems for plants. The chloride toxicity symptoms are leaf burns, leaf tissue deaths and early leaf drop (Ayers and Westcot 1985). The classification of irrigation water based on its chloride value is shown in Table 8. Although waters with chloride values below 140 mg/l are suitable for irrigation use, about 50% of water samples in the present study area had chloride values > 350 mg/l and severe hazard conditions for irrigation purposes.

Piper diagram

Piper in 1944 proposed a trilinear diagram to determine the geochemical evolution of groundwater. This diagram represents the chemistry of water samples. According to this procedure, the cations, i.e., calcium, magnesium and sodium plus potassium, and anions, i.e., sulfate, chloride and carbonate plus hydrogen carbonate, are presented in two distinct triangle plots. The result is then projected onto a diamond, which is a matrix transformation of a graph of the anions (sulfate + chloride/total anions) and cations (sodium + potassium/total cations) (Piper 1944). Figure 11a shows the Piper diagram of the water samples. It indicates that about 93% of the samples fell in sodium–chloride–sulfate facies, while 5% and 2% of the samples fell within calcium–magnesium–sulfate–chloride and sodium–bicarbonate facies, respectively (Fig. 11a). In addition, in more samples sodium and chloride were as dominant cations and anions with a frequency of 98% and 93%, respectively (Fig. 11b). Thus, most of the locations in the studied area fell under sodium–chloride–sulfate facies due to the presence of subsurface evaporative layers (Fig. 11c). It denotes that almost whole water samples in this region were alkaline water type with prevailing chloride (Ravikumar, Somashekar et al. 2015).

US salinity diagram (USSL 1954)

The US salinity diagram (USSL) is another hydrochemistry plot to evaluate the water suitability samples for irrigation purposes using EC and SAR values (US Salinity Laboratory (USSL) 1954). According to this diagram, groundwater quality was classified into sixteen classes (Table 9).

Based on the plot of groundwater data (Fig. 12a), most of the water samples in the study area have high EC and SAR values. Table 10 presents that 65.45% of samples are C4S4 type and 23.64% are C4S3 type with very high-salinity–high-sodium and very high-salinity–high-sodium hazards, respectively. The rest of samples are classified

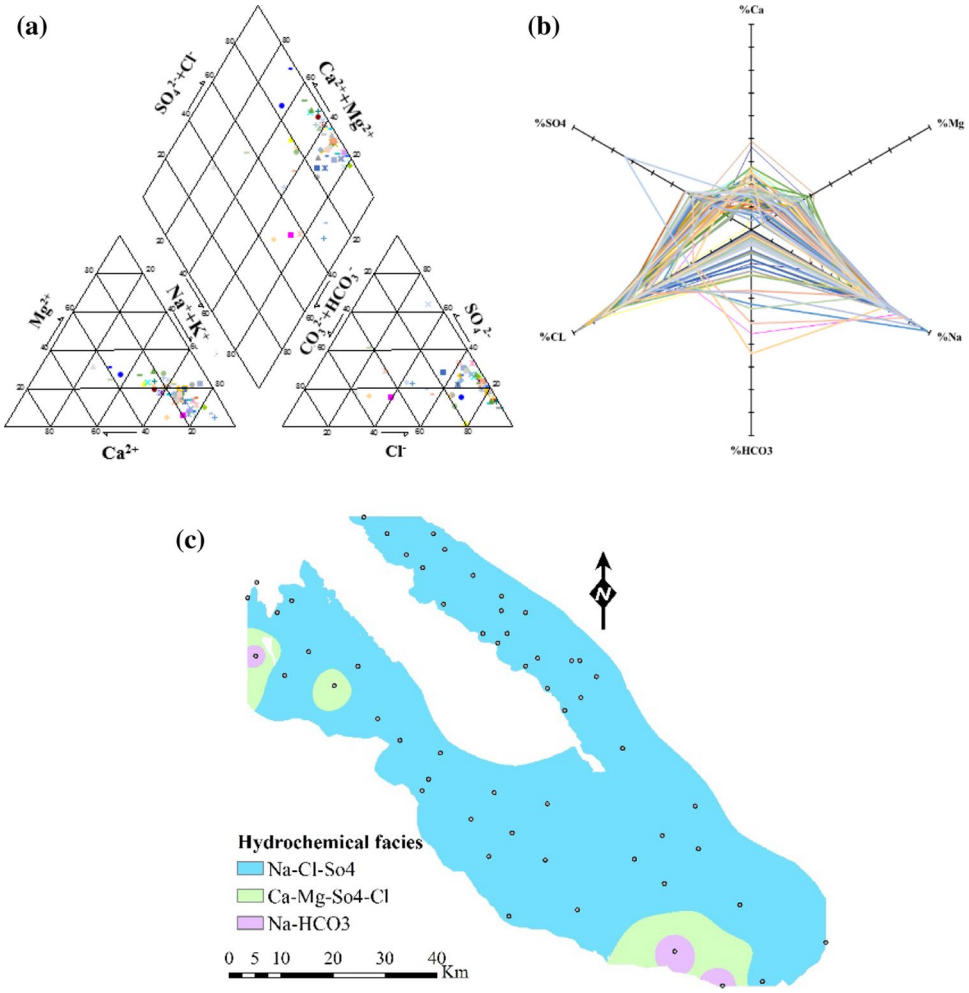

Fig. 11 **a** Piper diagram; **b** radial diagram; **c** spatial distribution of the water type/hydrochemical facies for 55 water samples

Table 9 Water classification for agricultural uses according to US Salinity classification (US Salinity Laboratory (USSL) 1954, Alavi, Zaree et al. 2016)

Class	Water quality for agriculture
C1S1	Sweet—completely ineffective for agriculture
C1S2-C2S2-C2S1	Brackish—approximately perfect for agriculture
C1S3-C2S3-C3S1-C3S2-C3S3	Passion—usable for agriculture
C4S1-C4S2-C4S4-C4S3-C1S4-C2S4-C3S4	Very passion—harmful to agriculture

as C4S2 (1.82%), C3S3 (1.82%), C3S2 (5.45) and C2S1 (1.82%). However, using very passion groundwater type for agricultural use causes different levels of soil salinity and sodicity hazards that applying salt leaching and reclamation techniques can be effective in improving plant growth and crop productivity (Bastani and Hosseininia 2018).

Wilcox diagram (Wilcox 1955)

Wilcox (1955) represented a diagram (using EC and Na%) with five classes including: excellent to good, good to permissible, permissible to doubtful, doubtful to unsuitable and unsuitable, in order to assess the water suitability for irrigation uses (Fig. 12b). This diagram reveals four, four and one groundwater samples in permissible to doubtful, doubtful to unsuitable and unsuitable classes, respectively. The remaining water samples had EC and TDS of more than 3500 µS/m and 35 mg/l, respectively, that they were unsuitable for irrigation purposes. The spatial distribution map shows that except for a few locations at the southeast corner of the studied area, all other parts were categorized as unsuitable (out of the Wilcox diagram) with high salinity values and sodium percentages (Fig. 12b and Fig. 13).

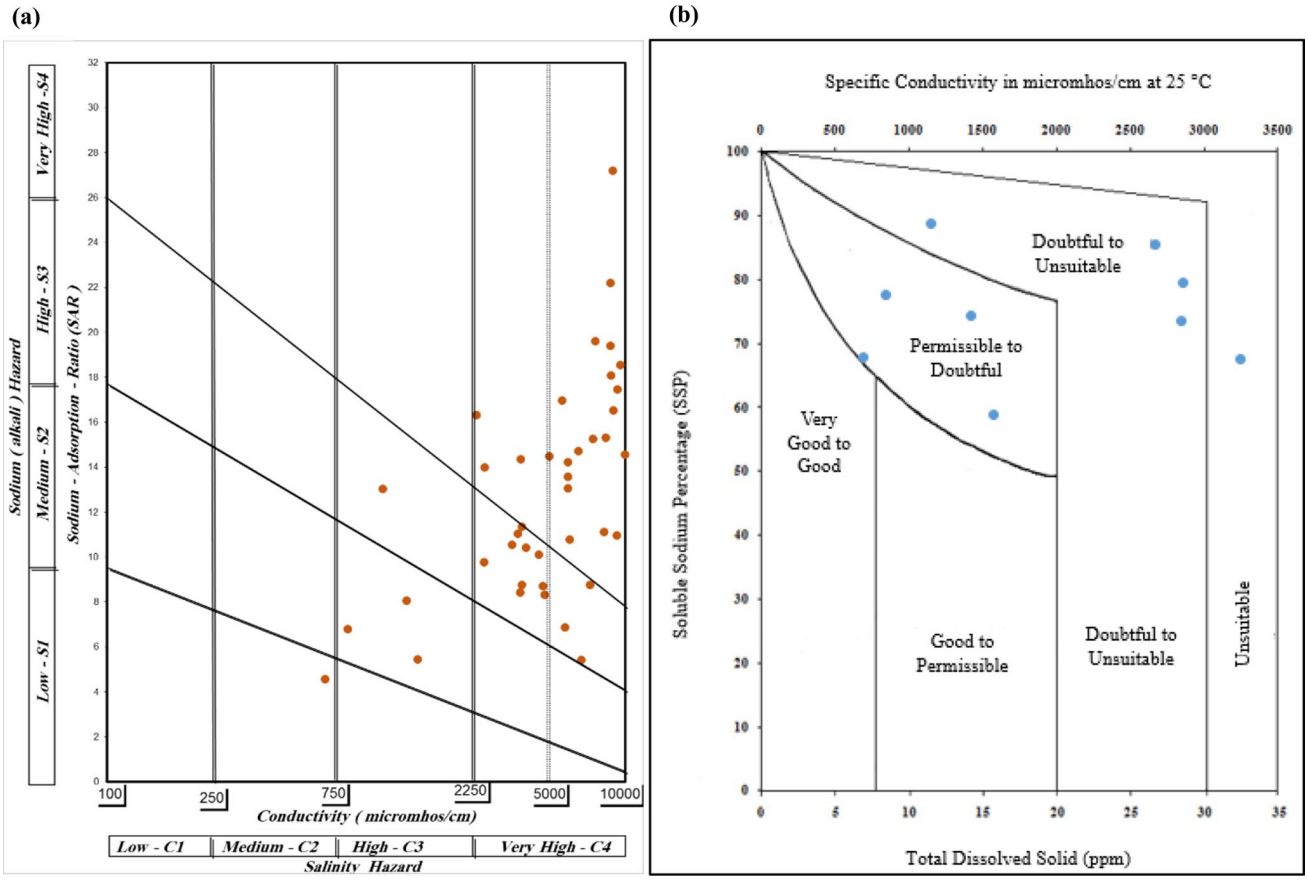

Fig. 12 **a** US salinity diagram; **b** Wilcox diagram for 55 water samples

Table 10 Categorization of groundwater based on US salinity diagram for 55 water samples

		Low	Medium	High	Very high
		S1	S2	S3	S4
Low	C1	-	-	-	-
Medium	C2	1.82	-	-	-
High	C3	-	5.45	1.82	-
Very high	C4	-	1.82	23.64	65.45

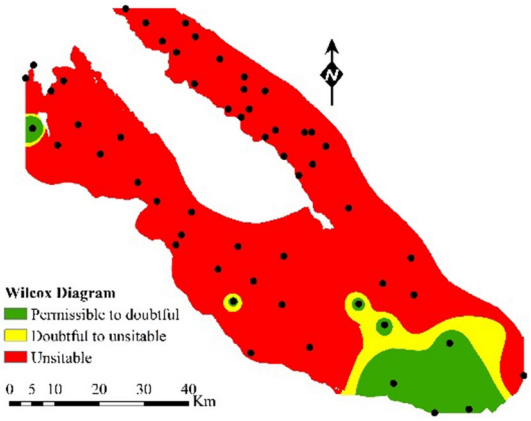

Fig. 13 Categorization of groundwater based on Wilcox diagram for 55 water samples

Conclusions

The assessment of the hydrogeological status of the study area in Rafsanjan plain, Iran was performed based on different approaches, namely drinking water standards, water quality index (WQI) and Schoeller diagram for domestic usage and irrigation water quality (IWQ) parameters, Piper diagram, US salinity diagram and Wilcox diagram for irrigation purpose. Accordingly, the main findings were categorized below:

- The average pH and EC values of groundwater were 7.02 and 8041.4 µS/m, respectively, which indicated neutral and saline water status.

- The GIS-based maps showed that variation of EC, TDS, TH and major ions in groundwater was strongly affected by groundwater flow and the geological structure of the studied area. A considerable increase in the mentioned parameters value was noted in the locations in the north and northeast of the studied area. Passing water flow through the evaporative deposition layers is the main reason for the rapid increase in the concentration of ions.
- According to WHO and ISIRI1053 standards, the concentrations of cations and ions and the values of EC, TDS and TH were significantly higher than acceptable limits and were critical for drinking purposes.
- WQI values classified the groundwater into good (1.8%), poor (3.6%), very poor (1.8%) and not suitable (92.7%) for drinking uses, based on WHO standards. According to ISIRI1053, the classification of groundwater for drinking indicated that 5.5%, 3.6%, 3.6% and 87.3%, of the samples in good, poor, very poor and not suitable classes, respectively.
- The Schoeller diagram illustrated that most of the water samples fell within the limits of 'bad' and 'in emergency' zones. The spatial distribution map demonstrated that the groundwater was rated as acceptable in a few locations in the southeast corner of the region; at the same time, the water quality drastically decreased toward the north and northwest area of the plain.
- IWQ parameters expressed that 85%, 67%, 32%, 51%, 43% and 50% of samples had EC > 3000, Na% > 60%, MAR > 50%, KR > 1, SAR > 9 and Cl^- > 350, respectively, which were unsuitable for irrigation uses. According to RSC and PI, about 91% of the groundwater samples had negative RSC value with little risk of sodium accumulation, and 69% of the samples belonged to suitable permeability conditions for long-term irrigation usage.
- The groundwater types were NaClSO4 (93%), CaMgSO4Cl (5%) and NaHCO3(2%), which denoted alkaline water type with prevailing chloride in most sites.
- Plots on US salinity diagram revealed that 63% of the water samples fell in very high-salinity–high-sodium hazard zones, while there were limited samples in the low-salinity or sodicity class. Thus, conducting some practices in order to reduce soil salinity and sodicity hazards can be effective in improving the conditions of irrigated lands and crop productivity.
- According to the Wilcox diagram, only 7% of groundwater samples were permissible to doubtful for irrigation, and the rest were doubtful (7%) to unsuitable (85%) classes, which existed in the central to northeast regions.
- Based on the results, it was concluded that almost all the groundwater samples were unsuitable for drinking and irrigation usage. Thus, some practices are recommended to reduce groundwater salinity in this area, such as: limiting over-exploitation of groundwater resources, controlling agricultural development and practices, using soil and water amendments, mixing high-salinity water with stored rainwater and applying modern irrigation methods and organic fertilizer (Etikala, Adimalla et al. 2021).

Acknowledgements The authors highly appreciate Kerman Regional Water Company and Graduate University of Advanced Technology for their support.

Funding The author(s) received no specific funding for this work.

Declarations

Conflict of interest The authors declare that they have no conflict of interest.

References

Asar Ab, 2019, The evaluation of water quality monitoring network of Kerman Province: Geology and Geohydrology report, Kerman Regional Water Company, 409p.

Abbasnia A et al (2019) Evaluation of groundwater quality using water quality index and its suitability for assessing water for drinking and irrigation purposes: case study of Sistan and Baluchistan province (Iran). Hum Ecol Risk Assess Int J 25(4):988–1005

Alavi N et al (2016) Water quality assessment and zoning analysis of Dez eastern aquifer by Schuler and Wilcox diagrams and GIS. Desalin Water Treat 57(50):23686–23697

Almodaresi SA et al (2019) Qualitative analysis of groundwater quality indicators based on schuler and Wilcox diagrams: IDW and Kriging models. J Envir Health Sustain Develop 4(4):903–912

Aminiyan MM, Aminiyan FM, Heydariyan A, Sadikhani MR (2016) The assessment of groundwater geochemistry of some wells in Rafsanjan plain. Iran Eur J Soil Sci 5(3):221–230

Arabpour and Adelpour, 2016, Evaluation of Exploration and Pizometric wells' log in Kerman Province, Kerman Regional Water Company, 581p.

Arota A et al (2022) Groundwater quality mapping for drinking and irrigation purposes using statistical, hydrochemical facies, and water quality indices in Tercha District, Dawuro Zone, Southern Ethiopia. J Degrad Mining Lands Manag 9(2):3367–3377

Ayers RS. and Westcot DW (1985). Water quality for agriculture, Food and Agriculture Organization of the United Nations Rome.

Baghalian K et al (2008) Effect of saline irrigation water on agronomical and phytochemical characters of chamomile (Matricaria recutita L.). Sci Hortic 116(4):437–441

Bastani S, Hosseininia M (2018) Efficiency analysis of localized leaching method to remove salts from the soil Case Study: pistachio orchard in Fath-Abad area of Kerman. Iran J Irrigat Drain 12(3):696–708

Chidambaram S et al (2022) Groundwater quality assessment for irrigation by adopting new suitability plot and spatial analysis based on fuzzy logic technique. Environ Res 204:111729

Choramin M et al (2015) Analyzing and studding chemical water quality parameters and its changes on the base of Schuler, Wilcox and Piper diagrams (project: Bahamanshir River). WALIA J 31(S4):22–27

Dehghani M (2011) Pollution of Anar Plain with Respect to Cadmium, Arsenic, Lead and Nitrate. Journal of Environmental Studies 36(56):87–100

Delgado C et al (2010) Quality of groundwater for irrigation in tropical karst environment: The case of Yucatan, Mexico. Agric Water Manag 97(10):1423–1433

Doneen, L. (1964). "Water quality for agriculture, Department of Irrigation." University of California, Davis: 48.

Ek AS, Renberg I (2001) Heavy metal pollution and lake acidity changes caused by one thousand years of copper mining at Falun, central Sweden. J Paleolimnol 26(1):89–107

Etikala B., et al. (2021) "Salinity Problems in Groundwater and Management Strategies in Arid and Semi-arid Regions." Groundwater Geochemistry: Pollut Remed Methods: 42–56.

Flowers TJ et al (2015) Sodium chloride toxicity and the cellular basis of salt tolerance in halophytes. Ann Bot 115(3):419–431

Hassanzadeh B, Abbassnejad A (2019) Hydrogeochemical processes affecting the quality of groundwater resources of the medial part of nuq plain (West of Kerman Province). Hydrogeology 3(2):46–58

Honarmand M, Khajehpour S, Shahriari H, Hoseinjani M (2017) Co-contamination of arsenic and other trace elements (Hg, Pb, Al, Fe, Cr, Ni, and Cd) in the Rafsanjan plain alluvial aquifer se of iran and arsenic risk assessment. Open J Geol 7(11):1710–1723

Hosseinifard SJ, Mirzaei Aminiyan M (2015) Hydrochemical characterization of groundwater quality for drinking and agricultural purposes: a case study in Rafsanjan plain, Iran. Water Qual Expo Health 7(4):531–544

Jamshidzadeh Z, Mirbagheri S (2011) Evaluation of groundwater quantity and quality in the Kashan Basin, Central Iran. Desalination 270(1–3):23–30

Kelly W (1957) Adsorbed sodium cation exchange capacity and percentage sodium sorption in alkali soils. Science 84:473–477

Khajepour, S. and Abbasnejad A (2007) Investigating the impact of Sarcheshme copper complex on the pollution of the groundwater in the south of Rafsanjan Plain. The 4th Conference on Geology and Environment.

Logeshkumaran A et al (2015) Hydro-geochemistry and application of water quality index (WQI) for groundwater quality assessment, Anna Nagar, part of Chennai City, Tamil Nadu, India. Appl Water Sci 5(4):335–343

Makki ZF et al (2021) GIS-based assessment of groundwater quality for drinking and irrigation purposes in central Iraq. Environ Monit Assess 193(2):1–27

Malakootian, M. and Khashi Z (2014) Heavy metals contamination of drinking water supplies in Southeastern villages of Rafsanjan plain: Survey of arsenic, cadmium, lead and copper.

Mirnezami SJ, Bagheri A, Maleki A (2018) Inaction of society on the drawdown of groundwater resources: a case study of Rafsanjan plain in Iran. Water Altern 11(3):725–748

Mohammadi AA et al (2017) Temporal and spatial variation of chemical parameter concentration in drinking water resources of Bandar-e Gaz City using geographic information system. Desalin Water Treat 68:170–176

Mohammadjani E, Yazdanian N (2014) Analysis of the state of the water crisis in the country and its management requirements. Quarterly Trend 21:117–144

Mosaferi M et al (2014) Quality modeling of drinking groundwater using GIS in rural communities, northwest of Iran. J Environ Health Sci Eng 12(1):1–14

Paliwal K (1972). "Irrigation with saline water, Monogram no. 2 (New series)." New Delhi, IARI **198**.

Palmajumder M et al (2021) An appraisal of geohydrological status and assessment of groundwater quality of Indpur Block, Bankura District, West Bengal, India. Appl Water Sci 11(3):1–21

Panahi G et al (2021) Physical–chemical evaluation of groundwater quality in semi-arid areas: case study—Sabzevar plain, Iran. Sust Water Resou Manag 7(6):1–15

Pansu, M. and Gautheyrou J (2007). Handbook of soil analysis: mineralogical, organic and inorganic methods, Springer Science & Business Media.

Piper AM (1944) A graphic procedure in the geochemical interpretation of water-analyses. EOS Trans Am Geophys Union 25(6):914–928

Piroozfar P et al (2018) Hydrogeochemical investigation and water quality assessment in the sarough watershed, Takab mining district. Geosci J 27(106):13–28

Pour HV et al (2014) Qualitative and quantitative evaluation of groundwater in Isfahan Najaf Abad Study Area. J Middle East Appl Sci Technol (JMEAST) 16:523–530

Prihar S et al. (1985). "Physical properties of mineral soils affecting rice-based cropping systems." Soil Physics and Rice, International Rice Research Institute, Los Banos, Philippines: 57–71.

Raghunath, I. (1987). "Groundwater, second." Wilely Easteren Ltd., New Delhi: 344–369.

Rahnama MB, Zamzam A (2013) Quantitative and qualitative simulation of groundwater by mathematical models in Rafsanjan aquifer using MODFLOW and MT3DMS. Arab J Geosci 6(3):901–912

Rajmohan N et al (2021) Assessment of groundwater quality and associated health risk in the arid environment, Western Saudi Arabia. Environ Sci Pollut Res 28(8):9628–9646

Raju NJ (2007) Hydrogeochemical parameters for assessment of groundwater quality in the upper Gunjanaeru River basin, Cuddapah District, Andhra Pradesh, South India. Environ Geol 52(6):1067–1074

Ravikumar P et al (2015) A comparative study on usage of Durov and Piper diagrams to interpret hydrochemical processes in groundwater from SRLIS river basin, Karnataka, India. Elixir Earth Sci 80(2015):31073–31077

Richards, LA (1954). Diagnosis and improvement of saline and alkali soils, LWW.

Sagar TV (2015) Water Quality of Some Polluted Lakes in GHMC Area, Hyderabad-India. Methodology 6:60–80

Salehi S, Esmaeily A, Farhadi H (2022) Determination of groundwater quality using a GIS-AHP based system and compared with Wilcox Diagram (Case Study: Rafsanjan Plain). Amirkabir J Civil Eng 54(1):283–298

Sawyer CN. and. McCarty PL (1967) "Chemistry for sanitary engineers."

Schoeller H (1977). "Geochemistry of groundwater." Groundwater studies, an international guide for research and practice, UNESCO, Paris: 1–18.

Silva M et al (2021) Assessment of groundwater quality in a Brazilian semiarid basin using an integration of GIS, water quality index and multivariate statistical techniques. J Hydrol 598:126346

Simsek C, Gunduz O (2007) IWQ index: a GIS-integrated technique to assess irrigation water quality. Environ Monit Assess 128(1):277–300

Singh J et al (2022) A hydrogeochemical approach to evaluate groundwater quality in the vicinity of three tributaries of the Beas River, North-West India. Appl Water Sci 12(1):1–18

Sonon, L., D. E. Kissel, P. F. Vendrell and R. Hitchcock 2007. Copper levels in drinking water from private household wells in major provinces of Georgia, Georgia Institute of Technology.

Srinivas Y et al (2013) Evaluation of groundwater quality in and around Nagercoil town, Tamilnadu, India: an integrated geochemical and GIS approach. Appl Water Sci 3(3):631–651

Tripathi A et al (2012) Assessment of groundwater quality Gurh Tehseel, Rewa District Madhya Pradesh, India. Int J Sci Eng Res 3(9):1–12

United States Public Health Service (USPH) (1962). Public health service drinking water standards, US Government Printing Office.

US Salinity Laboratory (USSL) (1954). Diagnosis and improvement of saline and alkali soils. , Agricultural handbook no. 60. USDA.

Vasanthavigar M et al (2010) Application of water quality index for groundwater quality assessment: Thirumanimuttar sub-basin, Tamilnadu, India. Environ Monit Assess 171(1):595–609

Water treatment physicochemical Specification of Iran (Tehran) (1997). Standard Organization and Iran Industrial Research (ISIRI),. Tehran.

WHO, G. (2011). "Guidelines for drinking-water quality." World health organization**216**: 303-304.

Wilcox L. (1955). Classification and use of irrigation waters, US Department of Agriculture.

Yousefi M et al (2018) Data on microbiological quality assessment of rural drinking water supplies in Poldasht county. Data Brief 17:763–769